

Characterizing correlations of flow oscillations at bottlenecks

Tobias Kretz, Marko Wölki, and Michael Schreckenberg
 Physik von Transport und Verkehr,
 Universität Duisburg-Essen,
 47057 Duisburg, Germany
 {kretz,woelki,schreckenberg}@traffic.uni-duisburg.de

December 23, 2021

Abstract

“Oscillations” occur in quite different kinds of many-particle-systems when two groups of particles with different directions of motion meet or intersect at a certain spot. In this work a model of pedestrian motion is presented that is able to reproduce oscillations with different characteristics. The Wald-Wolfowitz test and Gillis’ correlated random walk are shown to include observables that can be used to characterize different kinds of oscillations.

1 Introduction

The widely used word *oscillation* is defined for this article in a very general sense as the phenomenon that the direction of flow changes in certain intervals when two groups of particles compete for the chance to move at a narrow bottleneck. Oscillations in pedestrian dynamics have been dealt with before (see [1] for example). The aim of this work however is to give a framework for an analytical and quantitative treatment of oscillations in observation, experiment and simulation, which has not been done before. There are three extreme types of oscillation: 1) the zipper principle: the flow direction changes after each particle. 2) no oscillations: the flow direction only changes after one group has completely passed through the bottleneck. 3) uncorrelated oscillation: the statistics of the flow direction is the same as for coin-tossing experiments. While in the first two scenarios the whole process is completely determined as soon as the first particle has passed the bottleneck, there is absolutely no influence from one *event* to the next in the third scenario. Between those extremes there is a continuous spectrum of correlated oscillations with an influence from one event to the other but no full determination. The outline of the paper is as follows: First we present the parts of our model of pedestrian motion that are crucial for oscillations. We then describe the test scenario in detail. The third step is the presentation of the observables that characterize

a discrete oscillation. Finally we present the simulation results for different sets of parameters.

2 The model

A model of pedestrian motion is presented now that expands the model of [2, 3] for velocities $v > 1$ and adds some more features. Here we will only present the elements of the model that are involved in the phenomenon of oscillations. The full model in all details will be presented elsewhere [4]. The model is discrete in space (*cells*) as well as in time (*rounds*). Space is discretized into a regular lattice with cells with border length 40 cm. Each cell may be occupied by at most one *agent* as we will call the representation of a real person in the model. At the beginning of the simulation the distance of each cell to each exit is calculated and stored in the integer valued *static floor field* S_{xy}^e . So S_{xy}^e is the distance of cell (x, y) to exit e . Additionally to the static floor field there is an also integer valued *dynamic floor field* $\vec{D}_{xy} = (D_{xy}^x, D_{xy}^y)$ which in our model is a vector field. Whenever an agent leaves cell (x, y) and moves to cell $(x+i, y+j)$ the vector (i, j) is added to the dynamic floor field at the position (x, y) . In between the rounds of the agents' motion the dynamic floor field is subject to diffusion and decay with the two components diffusing and decaying independently: each entry (positive or negative) in a component decays with probability δ and if it does not decay, it diffuses with probability α to one of the neighboring cells.

The agents can have different maximal velocities. This is implemented by the number of cells an agent is allowed to move into any direction during one round. As one round is interpreted as one second, typical velocities are two to five cells per round. See [5] for details. So for each agent a there is a set R^a of cells, which are unoccupied and visible (not hidden by a wall or another agent) and which can be reached during the next round. At the beginning of each round each agent a randomly chooses a *destination cell* (x_d^a, y_d^a) out of R^a . The probability for a cell (x, y) within R^a to be chosen as destination cell by an agent currently positioned at (x_0^a, y_0^a) is:

$$p_{x,y}^a \propto \exp \left(k_S^a S_{xy}^{e=f(a, x_0^a, y_0^a, x_e, y_e)} + k_D^a ((x - x_0^a) D_{x_0^a, y_0^a}^x + (y - y_0^a) D_{x_0^a, y_0^a}^y) \right) \quad (1)$$

Compared to the model variants in [6] where desired trajectories are calculated in advance, by applying the same update rules v_{max} times and then different possible ways to use that trajectory to reach the final cell are investigated, here only a desired destination cell is calculated and the actual movement process is not implemented as planning process but as “real” motion. Note especially the equality of all cells of R^a , where in principal the relative position of a cell to an agent does not matter.

The dynamic floor field therefore influences the motion via the scalar product with a possible direction of motion. $S_{xy}^{e=f(a, x_0^a, y_0^a, x_e, y_e)}$ means that in the presence of more than one exit the choice of an exit is a function of the number (group affiliation) and the position of the agent as well as the position of the exit. Here all agents are only allowed to use the exit on the other side of the bottleneck compared to their starting position.

After all agents have chosen their destination cell in parallel, the agents start to move sequentially. It is important to mention that on their way to their destination cell they execute *single steps* within the Moore neighborhood [7] which implies that for $v = 1$ one step within the Moore neighborhood is possible. The sequence of all single steps of all agents is fixed randomly at the beginning of the motion part of a round. Compared to the model treated in [8] there is an additional shuffle as an agent does not necessarily execute all his steps at once. Whenever an agent has stepped on a cell and moved on, the cell remains *blocked* for all other agents until the rest of the round. This represents the speed-dependent occupation of space during motion [9, 10, 6], which is essential for a realistic fundamental diagram. Within a Moore neighborhood an agent always chooses the cell which lies closest to his destination cell and which has not been blocked before by another agent. If there is no unblocked cell left which is closer to the destination cell than the current cell, the round ends for that particular agent. Therefore an agent can fail to reach his destination cell. If two or more agents choose the same cell as destination cell or need the same cell as part of their path to their destination cell in the calculations for this work simply the order of movement decides about the winner of such a “conflict”.

3 The scenario

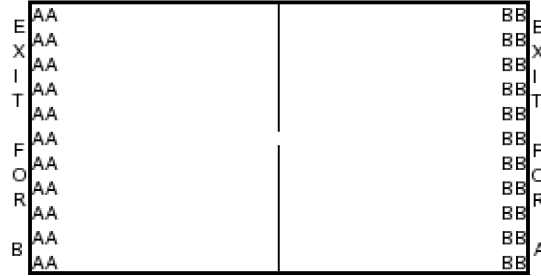


Figure 1: Initial positions of the agents in the scenario (schematic view).

At the beginning of the simulation two groups (A and B) with $N_A = N_B = 202$ ($N = N_A + N_B$) agents each are placed in two rows as shown in figure (1). They have to pass the bottleneck with a width of one cell in the middle and proceed to the exit on the other side. An agent is counted as having passed as soon as he leaves the bottleneck cell in the direction of his exit. The possibility that he moves back into the bottleneck is given but neglected. Only the first $n = 100$ agents passing the bottleneck are taken into account to make sure that there are always two almost equally sized groups competing for passage. Of these $n = 100$ agents the number of agents of group A is called n_A and of group B n_B . n can not be chosen arbitrarily large, as at some size the crowds in front of the bottleneck become that dense that no passing at all is possible.

There are no new agents entering the scenario.

4 Observables

4.1 The Wald-Wolfowitz test

The Wald-Wolfowitz test can be used to check for correlations in time series whenever the statistic is dichotomous or can be dichotomized, i.e. when two kinds of events or data are present. The probabilities for the events to happen do not need to be equal. In our case those two kinds of events are “A member of group A passes the bottleneck” and “A member of group B passes the bottleneck”. The Wald-Wolfowitz test makes a statement about the expectation value and the variance of the number of runs (and other observables) if there are no correlations between the different events. In the terminology of the test a *run* is a series of events of one kind not interrupted by an event of the other kind.

The crucial quantities of the Wald-Wolfowitz test are:

- $\langle R(n_A, n_B) \rangle$ is - for given n_A and n_B - the expectation value of the number of runs for an uncorrelated series of - in our case - bottleneck passages.
- σ_R is the standard deviation of the number of runs.
- r is the number of runs in a certain simulation,
- $z = \frac{r - \langle R(n_A, n_B) \rangle}{\sigma_R}$ is the standardized test variable.

For $n_A, n_B \gg 1$ (at least $n_A, n_B > 10$) the distribution of the number of runs becomes comparable to the normal distribution which implies that the null hypothesis “*The events are uncorrelated*” can be rejected on an α -level of significance if $|z| > q(1 - \alpha/2)$, with $q(1 - \alpha/2)$ as quantile of the standard normal distribution for the probability $1 - \alpha/2$. For smaller n_A, n_B one has to make use of tables to decide about the rejection of the null hypothesis [11, 12].

For an uncorrelated process one has for given n_A, n_B

$$\begin{aligned} \langle R(n_A, n_B) \rangle &= 2 \frac{n_A n_B}{n} + 1 = 2 \frac{n_A(n - n_A)}{n} + 1 \\ \sigma_R^2 &= \frac{2n_A n_B (2n_A n_B - n)}{n^2(n - 1)} = \frac{(\langle R \rangle - 1)(\langle R \rangle - 2)}{n - 1} \end{aligned} \quad (2) \quad (3)$$

The Wald-Wolfowitz test is independent of underlying distributions; therefore it does not make use of deviations in the distribution of n_A in subsequently repeated simulations of a scenario. This additional information can be made use of by mapping the process onto a correlated random walk.

4.2 Correlated random walk

In correlated random walk models [13, 14] the probabilities for the direction of the next step depend on the direction of the last step. The “correlated random walker” keeps his direction of motion with probability p and changes it with probability $1 - p$. In the first step the direction is chosen with equal probability. In the thermodynamic limit ($n \rightarrow \infty$) one then gets a normal distribution $\mathcal{N}(n/2, \frac{p}{1-p} \sigma_A^2(p = 0.5))$ for the

probability that the walker made n_A of n steps to the right [15]. Here $\mathcal{N}(X_0, \sigma^2)$ is the normal distribution with maximum at X_0 and variance σ^2 , and $\sigma_A^2(p = 0.5) = n/4$ is the variance for the number n_A of steps to the right in the case of uncorrelated random walk ($p = 0.5$). The position x_n of the walker after n steps is $n_A - n_B$. Numerical calculations (see figure 3 in appendix A) show that for $n = 100$ the thermodynamic limit is a good approximation (relative error for the standard deviation $< 1\%$) for $0.2 < p < 0.8$. The probability p to keep the direction should equal the sum of the correlation coefficients to find an event A directly followed by an event A and B directly followed by B .

$$p \approx cc_{\text{keep direction}} = cc_k = P(\langle AA \rangle_{\Delta events=1}) + P(\langle BB \rangle_{\Delta events=1}) \quad (4)$$

We map the events of the oscillation experiment on a special correlated walk – Gillis’ random walk in one dimension [16]:

- “An agent of group A passes the bottleneck.” \rightarrow “Random walker moves one step to the right.”
- “An agent of group B passes the bottleneck.” \rightarrow “Random walker moves one step to the left.”

Because of equation (2) there is a connection between $\langle R(n_A, n_B) \rangle$ - the expectation value of the number of runs - and σ_A . Since $\sigma_A = \sigma_B$ one has

$$\langle R(\sigma_A) \rangle \approx \frac{2}{n} \left(\frac{n}{2} + \sigma_A \right) \left(\frac{n}{2} - \sigma_A \right) + 1 = \frac{n}{2} + 1 - 2 \frac{\sigma_A^2}{n} \quad (5)$$

5 Values for an uncorrelated process

For $n = 100$ and $N_A = N_B = 202$ the expectation value for n_A has to be 50 ($= n/2$) due to the symmetry of the scenario. Even if a finite group size effect would in a strict sense imply a correlation, we here want to give not only the values for an uncorrelated process with no finite group size effect, but also for an else uncorrelated process with finite group size effect. In the first case, where the passing order can be imagined to be determined by a guardian at the bottleneck who decides about the right of passage of some member of one of the two groups by throwing a coin, the basic distribution is binomial. (All numerical values are calculated for $n = 100$ and $N_A = N_B = 202$)

$$P(n_A) = \binom{n}{n_A} 2^{-n} \quad (6)$$

$$\sigma_A = \frac{\sqrt{n}}{2} = 5 \quad (7)$$

$$\overline{\langle R \rangle} = \sum_{n_A=0}^n P(n_A) \langle R(n_A, n_B) \rangle = \frac{n}{2} + \frac{1}{2} = 50.5 \quad (8)$$

The latter case, where the guardian decides about the right of passage with equal probability for each of the remaining individuals, is governed by the hypergeometric distri-

bution.

$$P(n_A) = \frac{\binom{n}{n_A} \binom{N-n}{N_A-n_A}}{\binom{N}{N_A}} \quad (9)$$

$$\sigma_A = \sqrt{\frac{n}{4} \left(\frac{N-n}{N-1} \right)} = \sqrt{\frac{7600}{403}} \approx 4.34 \quad (10)$$

$$\overline{\langle R \rangle} = \frac{n}{2} + 1 - \frac{1}{2} \frac{N-n}{N-1} = 50 \frac{251}{403} \approx 50.62 \quad (11)$$

It is assumed that the size of groups on both sides of the bottleneck has no influence on the movement probability as long as both groups have some minimal size which should be exceeded by construction during the counting process as the largest possible inequality is 102:202. However even if this was not the case, this comparison shows that the expectation values of the two possible cases of an uncorrelated process differ only slightly. We now can take these results as basis for comparison to the results of our simulations.

6 Oscillations without dynamic floor field

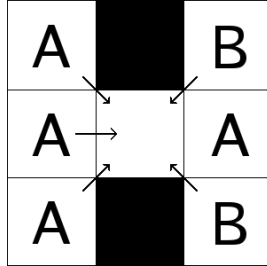


Figure 2: One of twelve possible situations after an agent has passed.

For $k_D = 0$ there is some sort of “intrinsic” correlation, which stems exclusively from the hard-core exclusion of the agents. As the last agent who passed, occupies one of the three cells which are adjacent to the bottleneck cell, there are on average fewer agents on the adjacent cells on the side of the group that could not move than on the other side. Figure 2 shows the situation when there is the maximum of three agents of the group that moved last and the maximum of only two agents of the other group. Of course there can be other combinations (3:2, 3:1, 3:0, 2:2, 2:1, 2:0, 1:2, 1:1, 1:0, 0:2, 0:1, 0:0) and the group that moved last can have fewer agents adjacent to the bottleneck, but on average there will be more. Therefore on that side there will on average also be more agents that plan to move to the bottleneck cell and so also the probability that one of them wins a possible conflict is increased, as the winner of a conflict is chosen with equal probability out of all competitors. Note that this effect crucially depends

on the choice of von Neumann neighborhood or Moore neighborhood as neighborhood for $v_{max} = 1$.

For $k_S = 0.5$ we repeated the calculations for the three cases $v_{max} = 1$, $v_{max} = 3$ and $v_{max} = 5$ one-hundred times each. The tables of this and the following section show the average number of runs that occurred, the average number of runs the Wald-Wolfowitz test predicts for uncorrelated behavior, average z-values as well as the number of times (out of 100) the z-value was smaller than -1.95 (5%-significance level) and smaller than -2.58 (1%-significance level), the standard deviation of n_A , the evacuation time (e.t.) in rounds and the probability to continue in the same direction as calculated from σ_A (p) as well as calculated from correlation coefficients (cc_k).

v	\bar{r}	$\overline{\langle R(n_A, n_B) \rangle}$	\bar{z}	5%	1%	σ_A	$\overline{e.t.}$	$p(\sigma_A)$	cc_k
1	37.04	50.51	-2.73	80	54	4.95	32945.9	0.49	0.64
3	37.47	50.26	-2.61	76	53	6.05	25676.0	0.59	0.63
5	37.94	50.36	-2.53	73	51	5.60	21395.4	0.56	0.63

Note that $\overline{\langle R(n_A, n_B) \rangle}$ is the average of the values for $\langle R(n_A, n_B) \rangle$ calculated from the 100 simulation results for n_A respectively n_B using equation (2) and averaged in the way it is done in equation (8) however using the distribution of simulation results and not a theoretical distribution $P(n_A)$. The other averages are also averages over 100 simulations.

7 Oscillations with dynamic floor field

For all simulations $k_D = 0.3$ and $k_S = 0.5$ has been set. This is quite a small value, however for $k_S = 1.0$ or even larger the crowds on both sides of the bottleneck become too dense, such that it becomes difficult for an agent to pass through them after he has passed the bottleneck. For each set of parameters the simulation was repeated 100 times. We mainly experimented with the maximum speed v_{max} (which was equal for all agents in a scenario) and the parameters for diffusion α and decay δ . The largest deviations from the uncorrelated case are marked in the following tables.

$v_{max} = 1, \delta = 0.03$									
α	\bar{r}	$\overline{\langle R(n_A, n_B) \rangle}$	\bar{z}	5%	1%	σ_A	$\overline{e.t.}$	$p(\sigma_A)$	cc_k
0.03	25.87	47.70	-4.69	98	95	12.84	5765.14	0.87	0.75
0.10	28.05	47.15	-4.15	94	84	13.84	6642.97	0.88	0.73
0.30	32.87	50.08	-3.52	93	86	6.75	13479.4	0.65	0.68
1.00	34.06	49.93	-3.26	90	75	7.32	13375.8	0.68	0.67

$v_{max} = 3, \delta = 0.03$									
α	\bar{r}	$\overline{\langle R(n_A, n_B) \rangle}$	\bar{z}	5%	1%	σ_A	$\overline{e.t.}$	$p(\sigma_A)$	cc_k
0.03	15.54	27.68	-3.86	74	69	34.06	2277.85	0.98	0.85
0.10	19.59	33.63	-4.09	81	73	29.47	2058.30	0.97	0.81
0.30	15.75	25.22	-3.61	74	65	35.79	1821.15	0.98	0.85
1.00	29.16	40.47	-2.86	74	58	22.94	2214.92	0.95	0.72

$v_{max} = 5, \delta = 0.03$									
α	\bar{r}	$\langle R(n_A, n_B) \rangle$	\bar{z}	5%	1%	σ_A	$\overline{e.t.}$	$p(\sigma_A)$	cc_k
0.03	21.60	25.86	-1.65	40	28	35.34	2063.88	0.98	0.79
0.10	20.85	31.29	-3.09	61	55	31.34	1758.01	0.98	0.80
0.30	17.68	27.58	-3.29	64	57	34.18	1519.78	0.98	0.83
1.00	28.22	36.51	-2.41	57	46	26.87	1730.61	0.97	0.73

(Also see figures 4, 5, 6, 7, 8 and 9 in appendix A.) Other simulations showed that for $\delta > 0.1$ the effect begins to vanish as the dynamic floor field decays too fast to have a significant influence and for $\delta < 0.01$ the effect is hidden by the dominant dynamic floor field that then induces irrational behavior. The agents begin to move in circles instead of heading to the bottleneck. Note that effects like this can also occur for too small α , if the dynamic floor field becomes too strong on some cells.

Compared to the case without dynamic floor field, the dynamic floor field with its time dependence brings in an another dimension that can be analyzed: As long as the dynamic floor field has not reached a steady-state, the oscillation will be time dependent. This implies that the measured values either change with n or if n is kept constant but the measurement process starts not with the first event but later. For $\alpha = 1.0$, $v_{max} = 1$ and $n = 150$ we got $z = -3.92$, which is quite a difference to $z = -3.26$ for $n = 100$. However except for the case $\alpha = 0$, where they became slightly larger, the correlation coefficients did not change at all. As the existence of time-dependent oscillation types is model-dependent, the analysis of this phenomenon shall not be done in further detail in this work.

8 Discussion

Some observations made in the $k_D = 0.3$ data are as follows.

- The evacuation time (in rounds) drops dramatically compared to $k_D = 0$ simulations. So it can be assumed that the larger groups of agents passing the door represent a more efficient behavior. This can be interpreted as less time being consumed by conflict solution processes at the bottleneck.
- The minimal z -value for each v_{max} is found at larger α for larger v_{max} . (See also figure 4.)
- The same holds for the minimum of the evacuation time. (See also figure 5.)
- Correlations manifest themselves for $v_{max} = 1$ typically in smaller z -values and for $v_{max} = 5$ typically in larger σ_A .
- σ_A for $v_{max} = 3$ and $v_{max} = 5$ are that large that $(n_A, n_B > 10)$ is not always fulfilled.
- For simulations with dynamic floor field, the correlations are stronger for $v_{max} = 3$ and $v_{max} = 5$ than for $v_{max} = 1$. This is due to the larger area of influence for higher speeds: more agents could choose the bottleneck cell as their destination cell. But due to the direction of the dynamic floor field mainly agents of the group that moved last indeed do choose the bottleneck cell as destination

cell, which leads to a stronger outnumbering of agents attempting to follow one of their group on the bottleneck cell compared to agents trying to change the direction of the flow, than in the case of $v_{max} = 1$.

- Also for simulations with dynamic floor field $p(\sigma_A)$ is most of the time much larger than cc_k , however within each v_{max} -set of results there appears to be a tendency that cc_k and p are positively correlated. The difference points to a dynamic floor field that is too strong to reverse direction with only one agent passing. If for example after a sequence of agents of group A one agent of group B passes the bottleneck, a typical sequence will look like $AAAAAABAAAA$ if the dynamic floor field does not change direction with that single agent. If however it does change, a typical sequence would be $AAAAAABBBBB$. In the first case σ_A will grow, as the dominance of agents of one group outlasts the accidental event with small probability that one agent of the other group passes. In the latter case σ_A will be comparatively small since one long run of A s can be followed by an equally long run of B s and vice versa. The correlation coefficient cc_k however is much less affected by this phenomenon as it is not distinguished between AA and BB sequences. Take for illustration an A - B -symmetric $n = 11$ example: ($AAAAAABAAAA$, $BBBBBBABBBB$) has $\sigma_A = 4.5$ and $cc_k = 0.8$ and ($AAAAAABBBBB$, $BBBBBBAAAAA$) has $\sigma_A = 0.5$ and $cc_k = 0.9$. So while σ_A becomes larger with a stronger dynamic floor field, cc_k becomes larger. Consequently did a simulation with $v = 3$, $\alpha = 1$ and $\delta = 0.1$ result in $cc_k = 0.64$ and $p = 0.61$ instead of $cc_k = 0.72$ and $p = 0.95$ as for the $\delta = 0.03$ simulation. This shows that a comparison of p and cc_k can give a hint that δ was chosen too small, as for real pedestrians the passing of one individual is enough to completely change the odds.
- Simulations without dynamic floor field gave values for σ_A and p that might make p look dependent of v . However the reason for this is a relatively broad distribution of the σ_A . In 20 additional $v_{max} = 1$ calculations of σ_A with $n = 100$ simulation repetitions each σ_A varied between $\sigma_A = 5.34$ and $\sigma_A = 6.72$ this implies values for p between $p = 0.53$ and $p = 0.64$ with an average of $p = 0.575$. At the same time cc_k remained relatively constant between $cc_k = 0.62$ and $cc_k = 0.64$. That p even at average remains smaller than cc_k probably results from a reduced local density directly in front of the bottleneck if a group had a sequence of agents passing the bottleneck. The reduced local density then increases the probability of a change of the flow direction. This is an effect of the kind of a hypergeometric distribution, that reduces the standard deviation (see above). Here too p is much more affected than cc_k as cc_k is not affected by the relative total numbers of A s and B s within the first n events, but only by the number of changes of the flow direction.

The significant drop in the evacuation time compared to $k_D = 0$ is a sign that the dynamic floor field not only leads to a more efficient motion into the bottleneck but also out of the bottleneck and through the group on the other side.

It is not very surprising, that the effects of the dynamic floor field are strongest for larger v_{max} at larger α , since the larger neighborhood in which faster agents can move

during one round makes it necessary that also the dynamic floor field diffuses faster to keep up with the agents.

If σ_A becomes too large, moderate z -values are no indicator that the events are uncorrelated. Contrary to that the scenario is just too small for such sets of parameters to make large z -values possible.

9 Summary, conclusions and outlook

A model of pedestrian motion was presented, which is able to modulate the characteristic observables of oscillations. The model was tested concerning this capability using the Wald-Wolfowitz test, a comparison to correlated random walks and a calculation of correlation coefficients. This framework for characterizing should be applicable to any model of pedestrian motion as well as corresponding experimental and empirical data. However these observables would show details that are far from having been measured in reality at present. Anyway the scenario of oscillations at bottlenecks did show up a rich variety of phenomena and observables, which might be used to characterize and distinguish models of pedestrian motion. The investigation of time-dependent oscillation types as well as the distribution of the length of runs could be further elements in such discussions. Observations and experiments in the field would be of great interest. Since our model is able to reproduce quite different types of oscillations it probably will also be able to reproduce the range of oscillations that occur in reality.

10 Acknowledgments

This work has been financed by the “Bundesministerium für Bildung und Forschung” (BMBF) within the PeSOS project. We would like to thank A. Schadschneider for comments and discussion.

References

- [1] D. Helbing and P. Molnar. Social force model for pedestrian dynamics. *Phys. Rev. E*, 51:4282–4286, 1995. `arXiv:cond-mat/9805244`.
- [2] C. Burstedde, K. Klauck, A. Schadschneider, and J. Zittarz. Simulation of pedestrian dynamics using a 2-dimensional cellular automaton. *Physica A*, 295:507, 2001. `arXiv:cond-mat/0102397`.
- [3] K. Nishinari, A. Kirchner, A. Namazi, and A. Schadschneider. Extended floor field CA model for evacuation dynamics. *IEICE Trans. Inf. & Syst.*, E87-D:726–732, 2004. `arXiv:cond-mat/0306262`.
- [4] T. Kretz. *Simulations of Pedestrian Dynamics*. PhD thesis, Universität Duisburg-Essen, 2006. to be published.

- [5] T. Kretz and M. Schreckenberg. Moore and more and symmetry. In Waldau et al. [18].
- [6] A. Kirchner, H. Klüpfel, K. Nishinari, A. Schadschneider, and M. Schreckenberg. Discretization effects and the influence of walking speed in cellular automata models for pedestrian dynamics. *J. Stat. Mech.*, P10011, 2004. [arXiv:cond-mat/0410706](https://arxiv.org/abs/cond-mat/0410706).
- [7] S. Wolfram. *Theory and Application of Cellular Automata*. World Scientific, Singapore, ISBN: 9971501236, August 1986.
- [8] M. Wölki, A. Schadschneider, and M. Schreckenberg. Asymmetric exclusion processes with shuffled dynamics. *J. Phys. A: Math. Gen.*, 39:33–44, 2006. <http://stacks.iop.org/0305-4470/39/33>.
- [9] H. Klüpfel. *A Cellular Automaton Model for Crowd Movement and Egress Simulation*. PhD thesis, Gerhard-Mercator-Universität Duisburg, 2003. <http://www.ub.uni-duisburg.de/ETD-db/theses/available/duett-08012003-092540/>
- [10] A. Seyfried, B. Steffen, W. Klingsch, T. Lippert, and M. Boltes. Steps toward the fundamental diagram - Empirical results and modelling. In Waldau et al. [18], page .
- [11] W. W. Daniel. *Applied nonparametric statistics*. Wadsworth Publishing, 2nd edition, 1989.
- [12] J. V. Bradley. *Distribution-Free Statistical Tests*, chapter 12, pages 271–282. Prentice Hall, 1968.
- [13] J. Gillis. Correlated Random Walk. *Proc. Camb. Phil. Soc.*, 51:639–651, 1955.
- [14] A. Chen and E. Renshaw. The Gillis-Domb-Fisher correlated random walk. *Journal of Applied Probability*, 29:792–813, 1992.
- [15] N. Konno. Limit theorems and absorption problems for one-dimensional correlated random walks. *ArXiv Quantum Physics e-prints*, October 2003. [arXiv:quant-ph/0310191](https://arxiv.org/abs/quant-ph/0310191).
- [16] N. Guillin-Plantard. Gillis’ random walks on graphs. *J. App. Prob.*, 42:295–301, 2005. URL: <http://projecteuclid.org/Dienst/UI/1.0/Summarize/euclid.jap/1110381390>.
- [17] M. Schreckenberg and S. D. Sharma, editors. *Pedestrian and Evacuation Dynamics*, Heidelberg, 2002. Springer.
- [18] N. Waldau, P. Gattermann, H. Knoflachner, and M. Schreckenberg, editors. *Pedestrian and Evacuation Dynamics ’05*, Heidelberg, March 2006. Springer.

A Figures

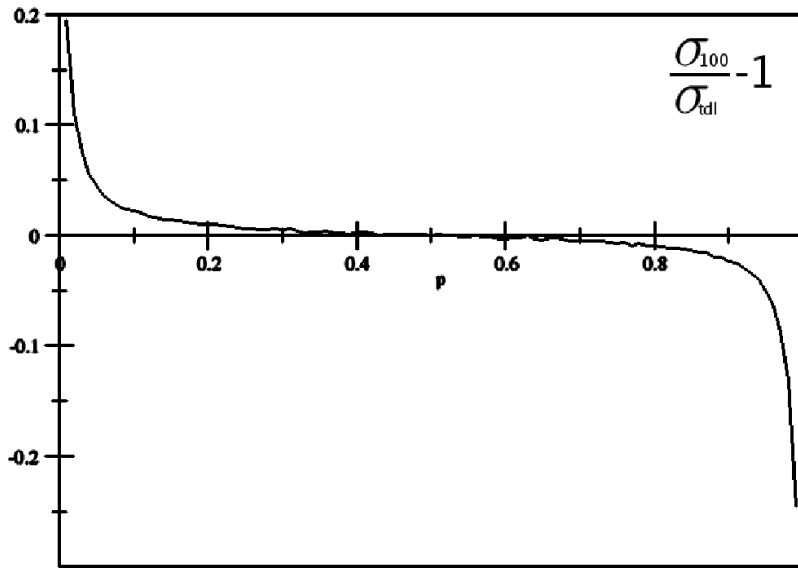


Figure 3: Relative difference of the numerically calculated standard deviation for the number of steps into a certain direction for $n = 100$ steps against the theoretical thermodynamical ($n \rightarrow \infty$) limit of the same standard deviation in dependence of the probability p to continue motion in the same direction.

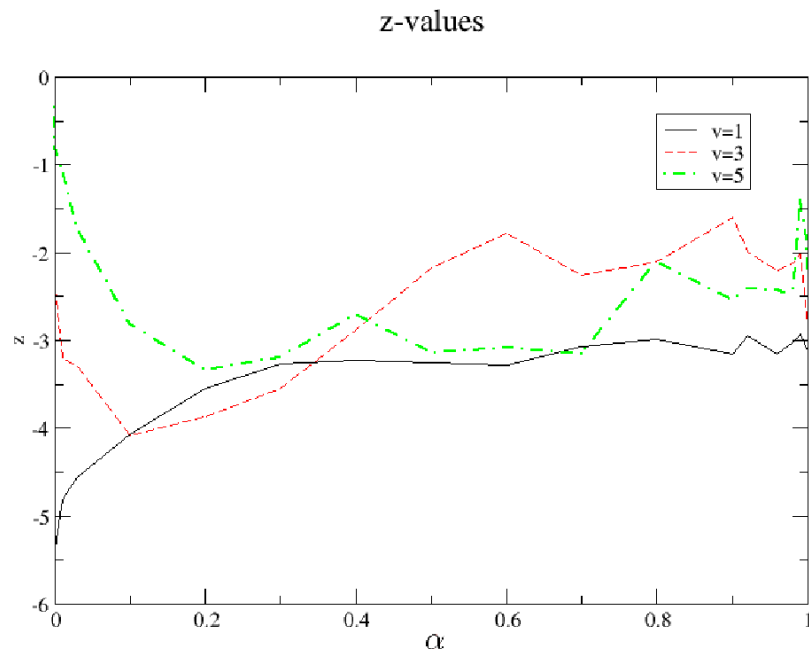


Figure 4: Average z -value for different α at $\delta = 0.03$.

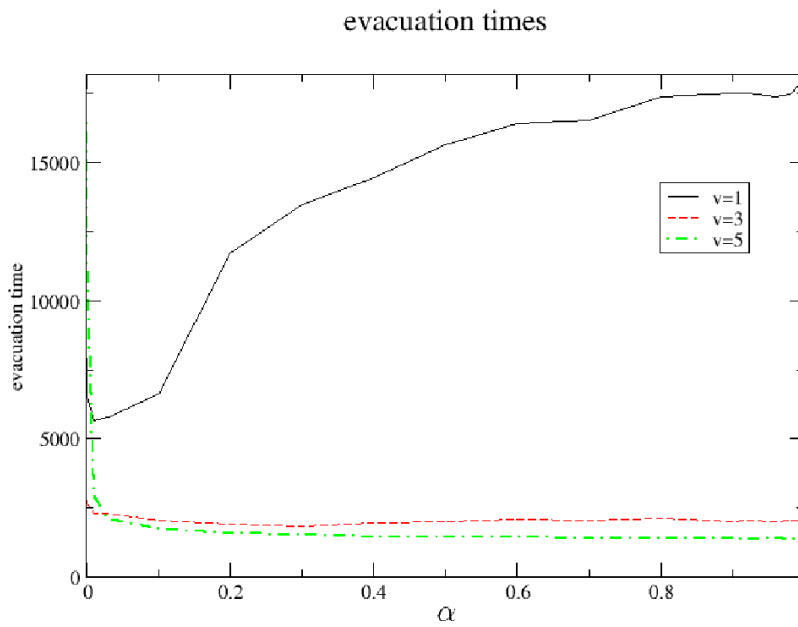


Figure 5: Average evacuation times for different α at $\delta = 0.03$.

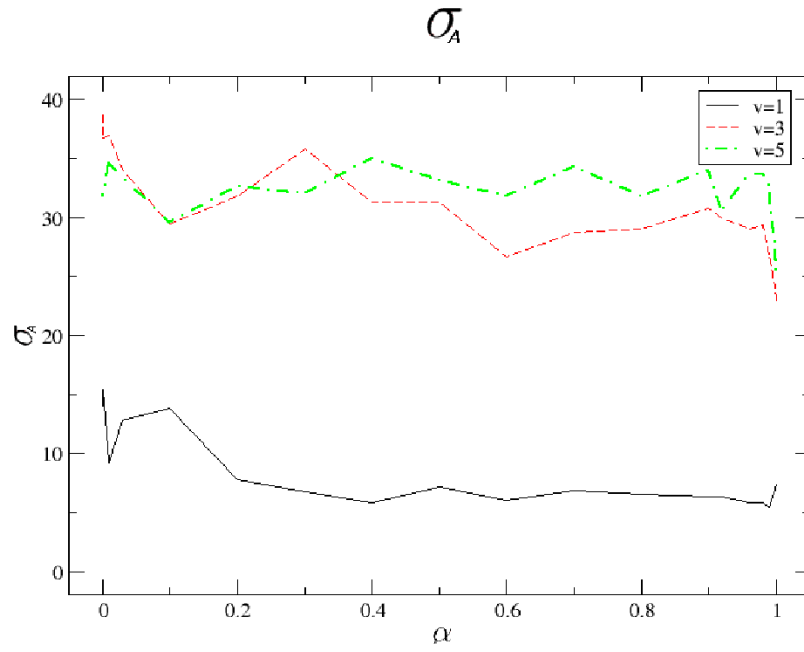


Figure 6: σ_A for different α at $\delta = 0.03$.

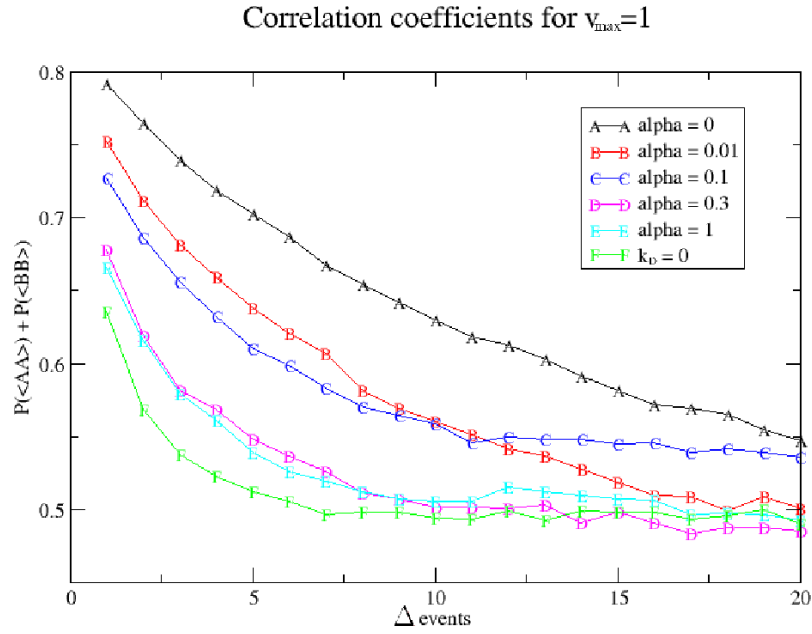


Figure 7: Correlation coefficients for different α and event distance at $v_{\max} = 1$

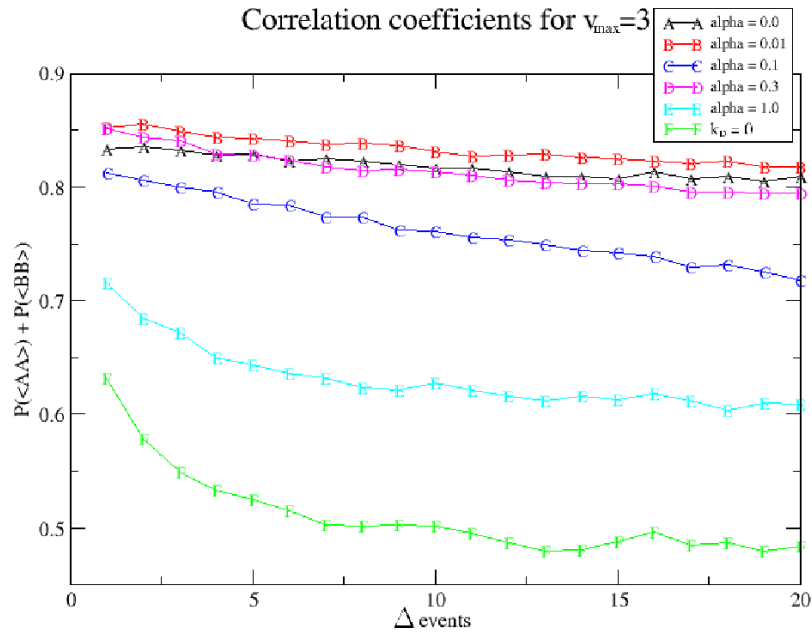


Figure 8: Correlation coefficients for different α and event distance at $v_{\max} = 3$

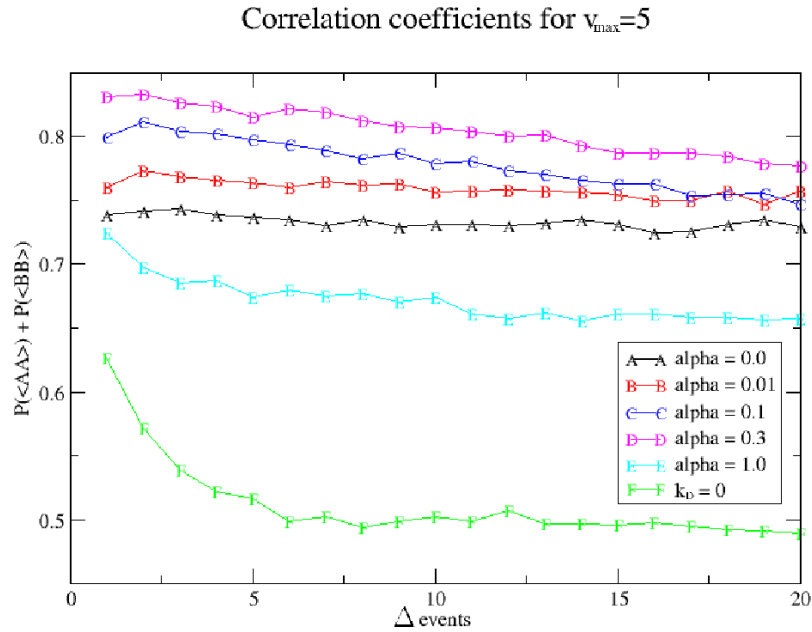


Figure 9: Correlation coefficients for different α and event distance at $v_{\max} = 5$.